Construction and Building Materials 239 (2020) 117824

Contents lists available at ScienceDirect

Construction and Building Materials

journal homepage: www.elsevier.com/locate/conbuildmat

Fatigue performance of long-term aged crumb rubber modified bitumen containing warm-mix additives

Haopeng Wang [a,*], Xueyan Liu [a], Martin van de Ven [a], Guoyang Lu [b], Sandra Erkens [a], Athanasios Skarpas [c,a]

[a] Faculty of Civil Engineering & Geosciences, Delft University of Technology, Delft, The Netherlands
[b] Institute of Highway Engineering, RWTH Aachen University, Aachen, Germany
[c] Department of Civil Infrastructure and Environmental Engineering, Khalifa University, Abu Dhabi, United Arab Emirates

HIGHLIGHTS

- This study compared different fatigue characterization methods for binders.
- Time sweep test measured fatigue life was compared with the linear amplitude sweep test predicted fatigue life.
- The effects of rubber content and warm-mix additives on the binder fatigue performance were investigated and analyzed.

ARTICLE INFO

Article history:
Received 21 September 2019
Received in revised form 24 November 2019
Accepted 6 December 2019

Keywords:
Crumb rubber modified bitumen
Warm mix asphalt
Fatigue
Time sweep
Linear amplitude sweep

ABSTRACT

Recently warm mix asphalt (WMA) technologies have been introduced to rubberized asphalt mixtures to decrease the required construction temperatures and to alleviate the hazardous gas emissions. Rubberized asphalt pavements combining with WMA have the potential to improve the long-term pavement performance. This study aims to investigate the fatigue performance of crumb rubber modified bitumen (CRMB) containing warm-mix additives using different characterization methods. The effects of crumb rubber modifier (CRM) content (5%, 10%, 15% and 22% by weight of base bitumen) and warm-mix additives on the binder fatigue performance were investigated. Various laboratory tests, including frequency sweep tests, time sweep (TS) tests and linear amplitude sweep (LAS) tests, were conducted on the long-term aged binders to obtain indicators of fatigue performance. Results show that there is a good correlation between the measured fatigue life determined by TS tests using the dissipated energy concept and the predicted fatigue life determined by LAS tests using the simplified viscoelastic continuum damage (S-VECD) theory. However, the traditional Superpave fatigue parameter and the G-R parameter cannot characterize accurate enough the fatigue performance of modified binders. CRMB binders exhibit superior fatigue performance compared to the neat bitumen. The effects of warm-mix additives on the fatigue performance are different for neat bitumen compared to CRMB binder. Based on the findings in this study, rubberized asphalt mixture combining with WMA additives is expected to have a promising long-term fatigue performance.

1. Introduction

1.1. Combination of crumb rubber modified bitumen and warm mix asphalt technology

With the developments in transportation and the associated increase in the number of vehicles, a huge amount of end-of-life tires (ELTs) are generated every year worldwide [1]. Scrap tires illegally disposed pose a potential threat to human health and increase environmental risks [2]. Due to the greater awareness of environmental issues and potential economic benefits, engineers are attempting to develop a more sustainable framework to dispose the ELTs. From a materials science point of view, the tire is made up of elastomeric compound, fabric and metal. The ELTs may be wastes for the tire industry, but they are still valuable raw materials for other applications. In civil engineering, bitumen modification with crumb rubber modifier (CRM) from ELTs, which is mainly the elastomeric compound, has been successfully applied in the paving industry since last century because of the economic benefits and environmental concerns [3]. Research has shown that the modification with CRM improves the rheological properties of

* Corresponding author.
E-mail address: haopeng.wang@tudelft.nl (H. Wang).

https://doi.org/10.1016/j.conbuildmat.2019.117824
0950-0618/

binders [4,5]. However, there are some concerns in using crumb rubber modified bitumen (CRMB) due to its high viscosity, such as poor pumpability, mixability and workability as well as the high heat energy consumption during the production stage in the asphalt plant. In addition, due to the requirements of higher mixing and compaction temperatures, the production of rubberized asphalt mixtures increases green gas emissions and produces more asphalt fumes and volatile organic compounds (VOCs). The compromised work conditions for labors at the construction site of rubberized asphalt pavement are also criticized [6]. Warm mix asphalt (WMA) technologies can help to decrease the construction temperatures of hot mix asphalt (HMA) through either reducing the viscosity, enhancing the lubricity or both [7–9]. The combination of rubberized asphalt and WMA technology is believed to be a promising and sustainable paving technology with many advantages, such as energy conservation, environmental protection, performance optimization and durability extension [10–12].

Fatigue cracking of asphalt pavements caused by repeated traffic loading at intermediate temperatures is a primary distress during the in-service period, which is an important factor to determine the durability of asphalt pavements. The fatigue performance of asphalt mixture is strongly related to the viscoelastic binder which determines the rheological, cohesive and adhesive behaviors of asphalt mixtures at different material scales [13,14]. Binders with good fatigue performance are beneficial for improving the fatigue resistance of asphalt mixtures. Therefore, accurate and effective characterization of the fatigue performance of CRMB with warm-mix additives is of great importance to optimize the mix design and to extend the service life of pavements with warm mix rubberized asphalt mixtures.

1.2. Fatigue characterization of binders using dynamic shear rheometer

The effective and accurate characterization of the fatigue performance of bituminous binders is important for binder grading and performance ranking and prediction [15]. The current Superpave performance grading (PG) specifications utilize the so-called fatigue parameter ($G^*\cdot\sin\delta$) to evaluate the binder's resistance to fatigue cracking. It is based on linear viscoelastic (LVE) properties of the RTFOT and PAV aged binder obtained from dynamic shear rheometer (DSR) at a frequency of 10 rad/s [16]. A major drawback of this fatigue parameter is that it cannot really account for real damage since it is determined within the LVE range of the binder where the nonlinear response is not captured [17]. Previous studies have shown that the parameter $G^*\cdot\sin\delta$ of binders has a low correlation with the fatigue performance of asphalt mixture and pavement. This is more evident for modified binders [18]. Recently, another rheological parameter $G^*\cdot(\cos\delta)^2/\sin\delta$ also based on the LVE properties from the DSR testing was proposed [19]. This parameter is called the Glover-Rowe (G-R) parameter, which can be calculated from frequency sweep test results at 15 °C and 0.005 rad/s. The G-R parameter was found to show a very strong correlation with binder ductility and can be used as an index for quantifying binder cracking resistance. A higher value of this parameter indicates increased brittleness or decreased ductility of binders [20]. While the G-R parameter correlates well with the cracking resistance of pavements with unmodified asphalt mixtures, whether it is still valid for polymer modified binders needs further research. In addition to the uncertainty of both fatigue parameters and G-R parameter for characterizing the fatigue resistance of modified binders, these two parameters have the following limitations: (1) both parameters are based on a single point measurement at one temperature and one frequency. Therefore, they provide no insights into the fatigue damage evolution and the effects of temperature and loading rates. (2) both parameters only consider the material response within the LVE range. Binders may experience much higher strain levels in the real pavement structure. In summary; these two parameters cannot account for the effect of the magnitude of traffic loading and link fatigue life to strain/stress levels.

To address the limitations of the above parameters, different test approaches and analysis methods were introduced to improve the fatigue characterization of binders. One of the introduced tests based on the same DSR measurement system to study the fatigue properties of binder is the time sweep (TS) test. Strain-controlled or stress-controlled repeated cyclic loading is applied on the binder specimen in the TS test at a fixed frequency and temperature [21]. The number of load cycles to failure at a prescribed stress or strain amplitude is usually used as an index to quantify the fatigue performance of the binder. Different fatigue failure definitions, e.g., stiffness reduction or physical failure, peak in phase angle, peak in $S \times N$ (stiffness times loading cycles), dissipated energy concept, etc., are proposed for fatigue analysis [22,23]. Particularly, the dissipated energy (DE) parameters [24] have been widely used to identify the fatigue failure point to determine the binder fatigue life. It was reported that TS test results can be effectively related to field performance under fatigue [25]. The obvious shortcomings of TS include the uncertainty of instability flow which interferes the fatigue analysis and the long testing time. Under this circumstance, the linear amplitude sweep (LAS) test was developed to accelerate the binder fatigue process. This test procedure also involves cyclic loading on a binder specimen at a constant temperature and frequency with the DSR, but with an increasing strain amplitude in a stepwise manner. Simplified viscoelastic continuum damage (S-VECD) theory was used for LAS test results analysis and prediction of binder fatigue life at any strain amplitude of interest. Similar to the TS test, the fatigue failure point needs to be clearly defined to allow for the prediction of fatigue life. The proposed thresholds of fatigue failure in the LAS test includes 35% reduction in so-called material integrity (as represented by $G^*\cdot\sin\delta$), peak in phase angle, peak in shear stress, and peak of $C \times N$ (material integrity times loading cycles) [26]. More recently, a pseudo-strain energy (PSE) based failure definition and criterion have been developed and implemented into the S-VECD modelling to predict the binder fatigue life [27]. It was found that the binder fatigue life predicted from LAS test results showed a promising correlation with the measured crack length in actual asphalt pavements of the Long-Term Pavement Preservation (LTPP) program [28]. Since the LAS test uses the same parallel-plate configuration with the DSR as the TS test, it also inherits similar drawbacks of the TS test, such as non-uniform shear stress distribution and instability flow at the edge [29]. This study attempts to characterize the fatigue performance of long-term aged CRMB with warm-mix additives using the above fatigue test methods with the DSR equipment. Different indicators of binder fatigue performance from different methods will be compared.

2. Objectives

The objectives of this study are: (1) to compare the fatigue performance indicators from different fatigue test methods; (2) to investigate the effect of CRM content and warm-mix additives on the fatigue performance of binders.

3. Experimental design

3.1. Materials

Penetration grade 70/100 bitumen (Nynas) was used as the base bitumen in this study. The base bitumen is graded as PG 64-22

according to the Superpave specification. The SARA (saturates, aromatics, resins and asphaltenes) fractions of the base bitumen are 7%, 51%, 22%, and 20% respectively. The CRM grains produced from scrap truck tires at ambient temperatures have an irregular shape. The fine CRM particle size ranges from 0 to 0.5 mm. The physical properties, composition and particle gradation of CRM are shown in Table 1. The processing agents mainly consist of antioxidants/antiozonants and curing additives (e.g., sulfur, zinc oxide, stearic acid, accelerator and oil etc.). Two types of non-foaming warm-mix additives, namely wax-based product W and chemical-based product C, were used in this study. Additive W is a synthetic hard wax that is free of sulphur and other impurities. The additive starts to crystallize at a temperature lower than 90 °C and forms a lattice structure. Additive C is a liquid cocktail of chemical products, such as surfactants, polymers, anti-stripping agents, etc.

3.2. Binder sample preparation

The CRMB binders were prepared in the laboratory by blending different percentages of CRMs with the base bitumen. Four CRM contents were used, respectively 5%, 10%, 15% and 22% by mass of base bitumen. The CRMBs were labelled as CRMB-5, CRMB-10, CRMB-15 and CRMB-22, linking to the amount of CRM added. CRMs were gradually added to the base bitumen accompanying with manual stirring for 5 min to ensure a good pre-distribution of CRMs. The blend was then mixed using a high shear mixer (Silverson) with a square hole screen. The mixing temperature was 180 °C and the mixing time was 30 min with a shearing speed of 6000 rpm. This mixing condition was determined based on the goal of optimizing the mechanical properties of CRMB [4]. During the blend mixing process, the mixer head was fully submerged into the hot bitumen to avoid oxidative ageing. To investigate the effect of warm mix additives on the fatigue properties of binders, two types of warm-mix additive were added into the base bitumen and CRMB-22 at 160 °C and manually mixed for 10 min. The resultant binders were designated as 70/100-W, 70/100-C, CRMB-22-W and CRMB-22-C. It should be noted that additives were only added to CRMB with a high percentage of CRM in an attempt to decrease its very high viscosity. The dosages of additives W and C were 2.0% and 0.6% respectively for both base bitumen and CRMB-22 based on the recommended dosage by the manufacturers and preliminary tests [4]. The mixing procedure is illustrated in Fig. 1. All the fresh binder samples were first short-term aged and then subjected to the pressure aging vessel (PAV) test in a pressurized environment (2.1 ± 0.1 MPa) at an elevated temperature of 100 °C for 20 h. Different DSR tests were conducted on these long-term aged binder samples to compare their fatigue performance.

Table 1
Basic properties and particle size distribution of CRM.

Properties		Description or value	
Source		Truck tyres	
Processing method		Ambient grounding	
Colour		Black	
Morphology		Porous	
Density (g/cm^3)		1.15 ± 0.05	
Decomposition temperature (°C)		~200	
Chemical composition	Total rubber (natural and synthetic)	55	
	Carbon Black (%)	25	
	Processing agents (%)	20	
Gradation	Sieves (mm)	Passing (%)	Retained (%)
	0.710	100	0
	0.500	93	7
	0.355	63	30
	0.180	21	42
	0.125	9	12
	0.063	2	7
	pan	–	2

3.3. Dynamic shear rheometer test

As described above, in total nine different binders are prepared to investigate the effects of warm-mix additives and CRM content on the fatigue performance of binders. The flow diagram of the experimental design for characterizing the fatigue performance is presented in Fig. 2.

3.3.1. Frequency sweep test

The rheological parameters (mainly complex shear modulus and phase angle) of different binders were measured with a DSR (Anton Paar). Frequency sweep (FS) tests were performed using the 25-mm parallel plate geometry with a 1-mm gap from 0.1 to 100 rad/s at temperatures of 10, 20, 30, 40 and 50 °C following the standard test procedure. All FS tests were conducted at a constant strain level of 0.1% to ensure the LVE response of binders. The Superpave fatigue parameter G*·sin δ and G-R parameter were extracted from the master curves established based on FS test results. Rheological parameters in the undamaged condition can also be obtained through FS tests.

3.3.2. Time sweep and linear amplitude sweep test

Both TS and LAS tests were carried out using the 8-mm parallel-plate and 2-mm gap configuration. Two replicates were tested for each testing scenario. As mentioned in previous studies, adhesive failure and unstable flow may occur during the fatigue test process under either low or high temperatures [30]. To measure true fatigue of the binder, the testing temperature for both TS and LAS tests were chosen at 20 °C, which produced the cohesive cracking with limited flow. The testing frequency was chosen as 10 Hz. Strain-controlled TS tests were conducted at strain levels of 2.5% and 5% which are able to obtain the rheological parameters in damaged condition. For the LAS test, the strain is increased linearly from 0.1 to 30% over the course of 3100 cycles of loading for a total test time of 310 s. Peak shear strain and stress, along with complex shear modulus and phase angle are recorded every 1 s (10 cycles of loading).

4. Analysis method

4.1. Linear viscoelasticity

In this study, a modified Christensen-Anderson-Marasteanu (CAM) model (Eqs. (1) and (2)) was adopted to build the master curves based on the FS test results [31].

$$G^* = \frac{G_g^*}{\left[1 + (f_c/f_r)^k\right]^{m/k}} \tag{1}$$

where G_g^* is the G^* when the frequency approaches to infinity, often called glass complex modulus; f_c is the crossover frequency; f_r is the reduced frequency; and k, m are the shape parameters, dimensionless.

$$\delta = 90\boldsymbol{I} - \frac{90\boldsymbol{I} - \boldsymbol{\delta_m}}{\left\{1 + \left[\frac{\boldsymbol{log}(\boldsymbol{f_d}/f_r)}{\boldsymbol{R_d}}\right]^2\right\}^{\boldsymbol{m_d}/2}} \tag{2}$$

where $\boldsymbol{\delta_m}$ is the phase-angle constant at $\boldsymbol{f_d}$, the value at the inflexion point for binders; $\boldsymbol{f_d}$ is the location parameter with a dimension of frequency, at which $\boldsymbol{\delta_m}$ occurs;$\boldsymbol{R_d}$, $\boldsymbol{m_d}$ are the shape parameters;

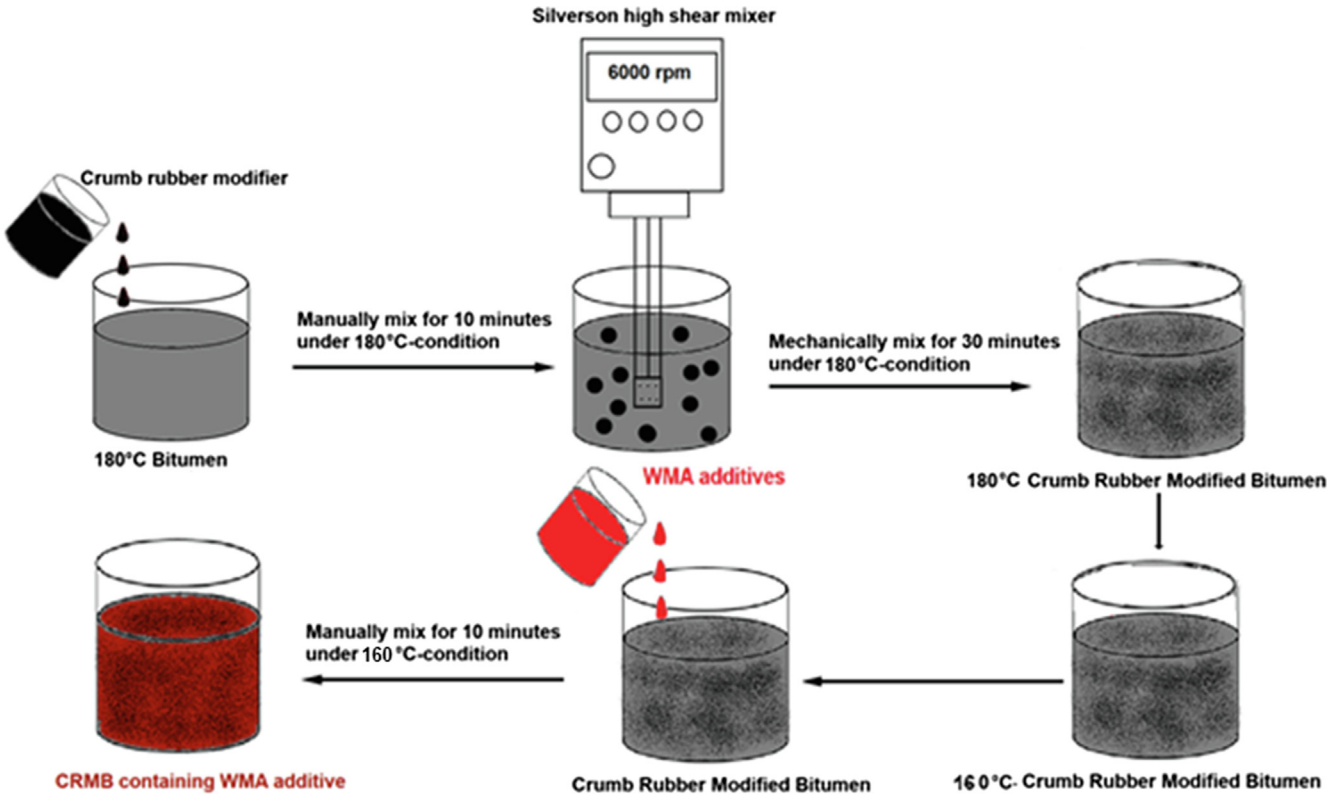

Fig. 1. Mixing procedure for preparing CRMB binders.

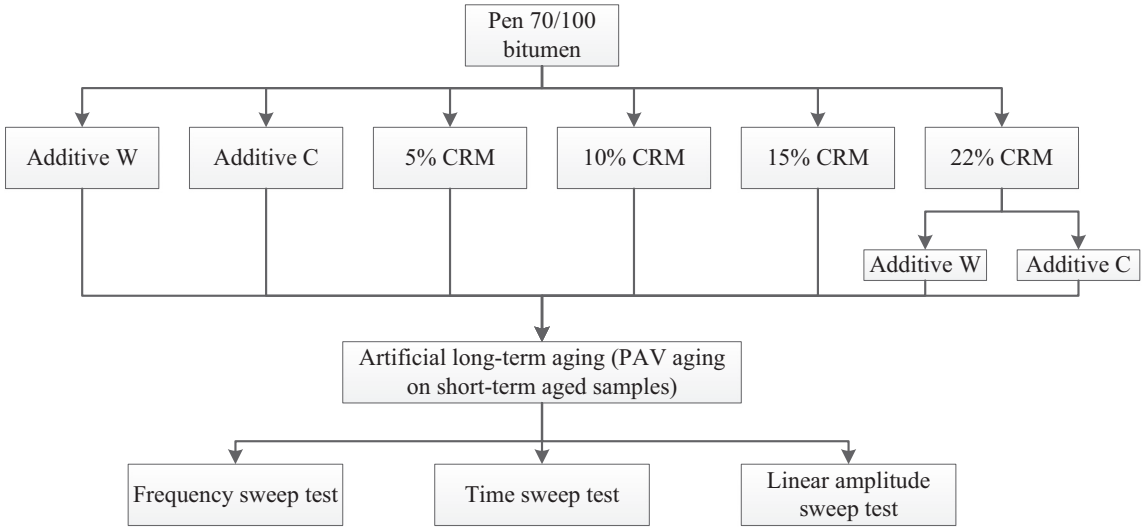

Fig. 2. Flow chart of experimental design for binder testing.

and for binders, $I = 0$ if $f > f_d$, $I = 1$ if $f \leq f_d$. The Williams-Landel-Ferry (WLF) equation (Eq. (3)) was used to obtain the shift factors.

$$\log \alpha_T(T) = \frac{-C_1(T - T_R)}{C_2 + (T - T_R)} \tag{3}$$

where C_1, C_2 are the empirically determined constants; T is the test temperature; T_R is the reference temperature; $\alpha_T(T)$ is the shifting factor.

4.2. Dissipated energy-based modelling of TS test

Fig. 3 shows the three main damage stages during the fatigue damage evolution of binders [24]. In the first stage, the dissipated energy (DE) for each cycle is constant and no damage occurs. In the second stage, the material integrity of binders is deteriorated gradually and crack initiates. In the crack propagation stage, a rapid change of material response is observed, and damage is accumulated in a more aggressive way until complete failure is reached.

Fig. 3. Fatigue damage evolution of binders.

The two transition points separating the three damage stages can be defined using the cumulative dissipated energy ratio (DER) concept as shown in Eq. (4).

$$\mathbf{DER}_n = \frac{\sum_{i=1}^{n} \boldsymbol{W_i}}{\boldsymbol{W_n}} \tag{4}$$

where $\boldsymbol{W_i}$ is the DE in a given cycle, which can be calculated using the stress and strain amplitudes in the ith cycle, $\tau_{0,i}$ and $\gamma_{0,i}$ with Eq. (5). $\boldsymbol{W_n}$ is the dissipated energy in the nth cycle.

$$\boldsymbol{W_i} = \pi\tau_{0,i}\gamma_{0,i}\sin(\delta_i) \tag{5}$$

The DER of each cycle is calculated using Eq. (4) and plot against the cycles of loading to monitor the fatigue evolution. For a strain-controlled TS test, the material deteriorates as the test progresses resulting in lower stress levels to maintain the constant strain amplitude. Therefore, with the increase of number of load cycles in a strain-controlled test, the DE in each cycle decreases while the DER steadily increases. In contrary to the stress-controlled TS test, there is no clear failure point for the strain-controlled test. A parameter referred as $\boldsymbol{N_{p20}}$ is proposed as a failure criterion. It is defined as the number of load cycles at which the DER deviates from the equality line by 20%. The parameter $\boldsymbol{N_p}$ in the plot corresponds to the intersection of two asymptotes. The relationship between fatigue life and the initial DE is described by a traditional power function (Eq. (6)) [24].

$$N_{p20} = K_2\left(\frac{1}{W_i}\right)^{K_1} \tag{6}$$

where K_1 and K_2 are the fitting parameters related to the energy input of binder and testing temperature [25]. Fig. 4 summarizes the evolution of the DER and the determination of N_{p20} in a strain-controlled TS test. Conceptually, the fatigue life of the binder defined as N_{p20} previously is represented by the cycles of loading required to undergo the crack initiation without reaching the crack propagation.

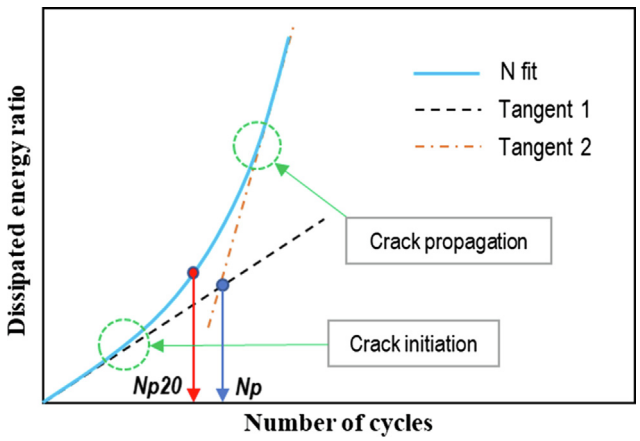

Fig. 4. Variation in the DER for a strain-controlled TS test.

4.3. Simplified viscoelastic continuum damage (S-VECD) modelling of LAS test

The LAS test results are interpreted using the S-VECD theory. An integrated S-VECD fatigue characterization framework is made up of three material functions, namely LVE property, damage characteristic curve, and fatigue failure criterion [32]. To quantify the damage in the VECD modelling, an internal state variable S is introduced based on Schapery's work potential theory [33] and can be derived from the damage evolution law:

$$\frac{dS}{dt} = \left(-\frac{\partial W^R}{\partial S}\right)^{\alpha} \tag{7}$$

where α is a material-dependent constant that represents the rate of damage accumulation; t is time; W^R is the pseudo-strain energy density. For this paper, the material parameter α is defined as $1/m + 1$ for binders, where m is the slope of the dynamic shear modulus master curve in the log space [34]. Pseudo-strain energy is defined as:

$$W^R = \frac{1}{2}DMR \cdot C(S)\left(\gamma^R\right)^2 \tag{8}$$

where DMR is the dynamic modulus ratio accounting for the specimen-to-specimen variability. The C is the pseudo stiffness to quantify the material integrity as defined in Eq. (9).

$$C(S) = \frac{\tau_p}{\gamma^R \cdot DMR} \tag{9}$$

where τ_p is the peak stress in a given cycle; γ^R is the pseudo strain amplitude in a given cycle which can be defined as in Eq. (10).

$$\gamma^R = \frac{1}{G_R}\left(\gamma_p \cdot |G^*|_{LVE}\right) \tag{10}$$

where G_R is an arbitrary reference modulus; γ_p is the strain amplitude in a given cycle; $|G^*|_{LVE}$ is the LVE dynamic shear modulus at the fatigue testing temperature and frequency. Combining the above equations, the damage at any time t (damage characteristic curve) can be derived in terms of material integrity as:

$$S(t) = \sum_{i=1}^{N}\left[\frac{DMR}{2}\left(\gamma^R\right)^2\left(C_{i-1} - C_i\right)\right]^{\frac{\alpha}{\alpha+1}} \cdot \left(t_i - t_{i-1}\right)^{\frac{1}{1+\alpha}} \tag{11}$$

where N is the cycles of loading and i refers to the cycle number. Since the relationship between $C(S)$ and S is independent of loading history, the S-VECD model is capable of back-calculating fatigue life under any loading condition of interest (e.g., strain level). To allow for fatigue life predictions, a power law model is fitted to the damage characteristic curve (Eq. (12)) [28].

$$C(S) = 1 - C_1 \cdot S^{C_2} \tag{12}$$

where C_1 and C_2 are model fitting parameters. Combining the above equations, the relationship between fatigue life N_f and strain amplitude can be derived as [27]:

$$N_f = \frac{f \cdot 2^{\alpha} \cdot S_f^{\,1-\alpha C_2+\alpha}}{(1-\alpha C_2+\alpha)(C_1 C_2)^{\alpha}\left(\gamma_p \cdot |G^*|_{LVE}\right)^{2\alpha}} \tag{13}$$

where S_f is the damage at failure point; f is the loading frequency.

5. Results and discussion

5.1. Superpave fatigue parameter and G-R parameter

Complex shear moduli and phase angles of different binders at various temperatures and frequencies were obtained from the frequency sweep tests. The values of the Superpave fatigue parameter and G-R parameter were calculated for different binders and shown in Figs. 5 and 6, respectively. A lower value of G*·sin δ is preferred to ensure better fatigue performance based on the Superpave specification. It can be seen from Fig. 5 that two types of warm-mix additives have different effects on the fatigue parameter of both neat bitumen and CRMB. Wax-based additive is detrimental to the fatigue resistance of the binder while the chemical-based additive improves fatigue resistance. It is obvious that CRMB binders possess higher fatigue resistance than neat bitumen. With the increase of CRM content, the G*·sin δ decreases, indicating an increase in binder elasticity and fatigue resistance at intermediate temperatures. However, only CRMB binders with a CRM content higher than 10% in this study meet the G*·sin δ requirement of not exceeding 5000 kPa at the PAV-aged condition and this particular temperature.

In terms of the G-R parameter, similar to the results of the fatigue parameter, warm-mix additives have opposite effects on the binder. The addition of wax-based additive makes the binder more brittle (higher stiffness/lower phase angle) while chemical-based additive has a softening effect on the binder. However, the modification with CRM increases the value of the G-R parameter of the binder, indicating a more brittle behavior. With the increase of CRM content, the ductility of the binder slightly increases as reflected by the decreased G-R parameter. If considering a G-R parameter value of 180 kPa as the point of damage onset, all the binders tested are still at the undamaged condition.

Based on the above results, the Superpave fatigue parameter and G-R parameter provide inconsistent findings on the fatigue performance of the binder. As mentioned before, both parameters

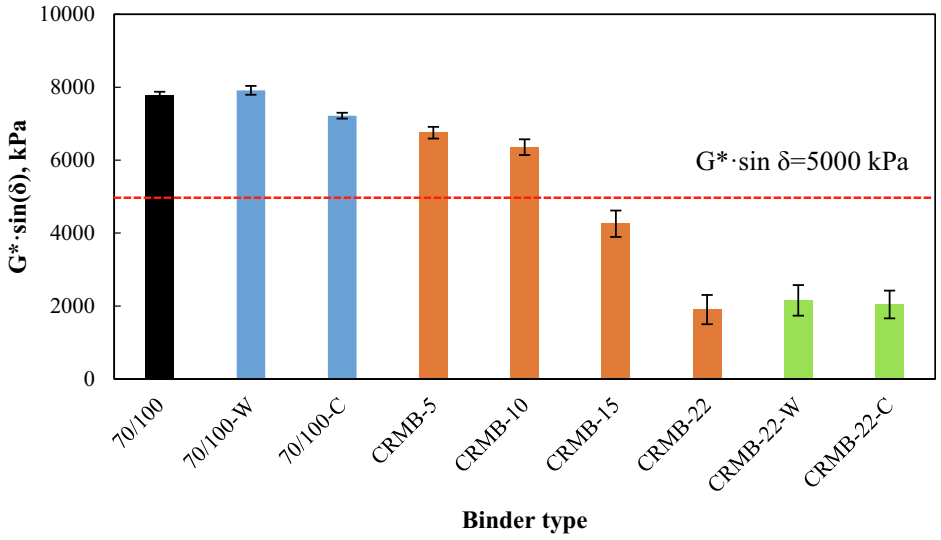

Fig. 5. Superpave fatigue parameters of different binders.

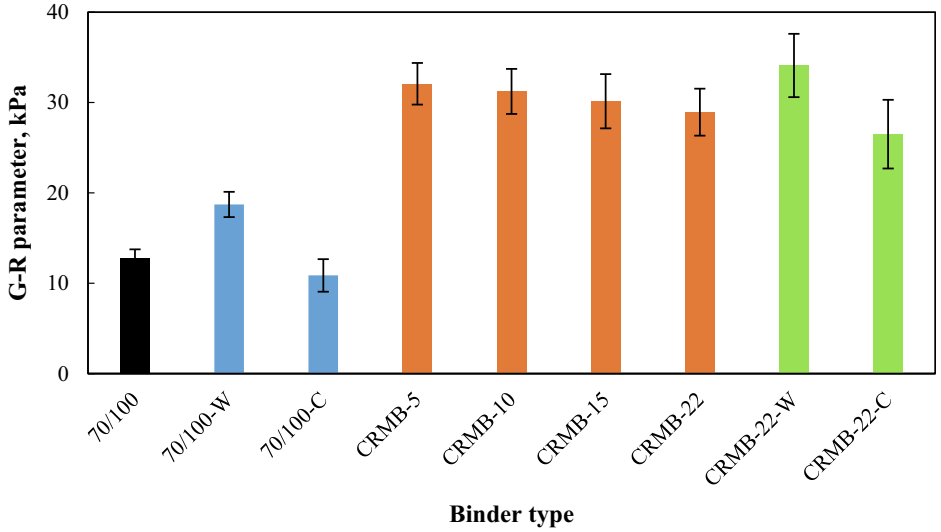

Fig. 6. G-R parameters of different binders.

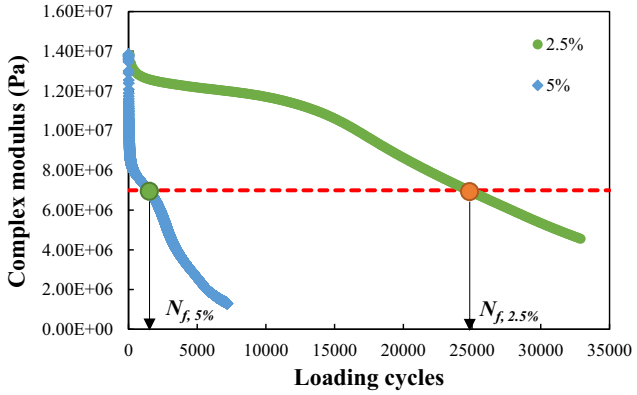

Fig. 7. Complex modulus evolution of neat bitumen 70/100 in the strain-controlled TS fatigue tests.

are based on the point values of complex shear modulus and phase angle at a certain temperature and frequency under a low strain loading condition. Therefore, fatigue damage evolutions of a binder under large-strain nonlinear range cannot be captured. TS tests and LAS tests were further conducted to investigate the fatigue performance of different binders.

5.2. Time sweep test

5.2.1. DER curve

The TS test was designed to quantify the binder fatigue resistance by monitoring the deterioration of the material integrity (usually modulus) under repeated loading. Fig. 7 presents a typical material response during the strain-controlled TS test of the neat bitumen 70/100. The other binders also showed similar trends thereof omitted here. It is obvious that the complex modulus of the binder deteriorates faster at the high strain level of 5% than 2.5%, resulting in a shorter fatigue life. The simplest fatigue failure definition for TS tests is the point corresponding to the 50% loss in stiffness. The red dashed line in Fig. 7 represents the approximate 50% reduction of the initial complex modulus of the neat bitumen. The corresponding loading cycles of the two crossover points are the fatigue life values at the two strain levels. However, this fatigue failure definition has been criticized since it is arbitrary and lacks theoretical verification [23]. Dissipated energy-based parameters were proposed to be more fundamentally related to fatigue failure. The DER approach was adopted to evaluate the fatigue property of binders and derive the fatigue law based on the TS results.

Fig. 8 shows the DER curves of different binders with the progress of loading cycles at the strain level of 2.5%. At the initial stage, all the binders display a linear increase of DER values with the increase of loading cycles. This stage is believed to be the no-damage stage as the dissipated energy contributes completely to the viscoelastic damping without any damage. As the cyclic loading progresses, the trendline of DER versus number of cycles deviates from the initial linear slope. The deviation point is regarded as the crack initiation point. After more damage cumulated as the testing carries on, the DER value will increase in a more rapid manner and the crack propagation point will be reached. In terms of the modification of CRM, it can be seen from Fig. 8a that CRMB binders show a wide range of results. Compared to the neat bitumen, a delayed crack initiation can be observed for the CRMB binders from Fig. 8a. For neat bitumen and CRMB binders with relatively low CRM content, the slope of the DER curves increase rapidly. The slope deviation from linearity was less pronounced for the CRMB-15 and CRMB-22 binders, indicating significant improvement in fatigue resistance. With regard to warm-mix additives, it seems that the wax-based additive causes earlier crack initiation compared to the neat bitumen while addition of chemical-based additive delays the crack initiation as shown in Fig. 8b. However, the DER curves are overlapping at the later stage. Therefore, the exact fatigue life of each binder needs to be further determined by modeling the test results. In contrast with the results for the neat bitumen, both types of warm-mix additives improve the fatigue resistance of CRMB-22 as shown in Fig. 8c.

5.2.2. Determination of fatigue life

To determine the binder fatigue life N_{p20}, the following model was used to fit the curve of DER versus number of load cycles [24].

$$N = N_c + b_1(R - R_c) + T(b_2 - b_1)\ln\left\{1 + e^{[(R-R_c)/T]}\right\} \quad (14)$$

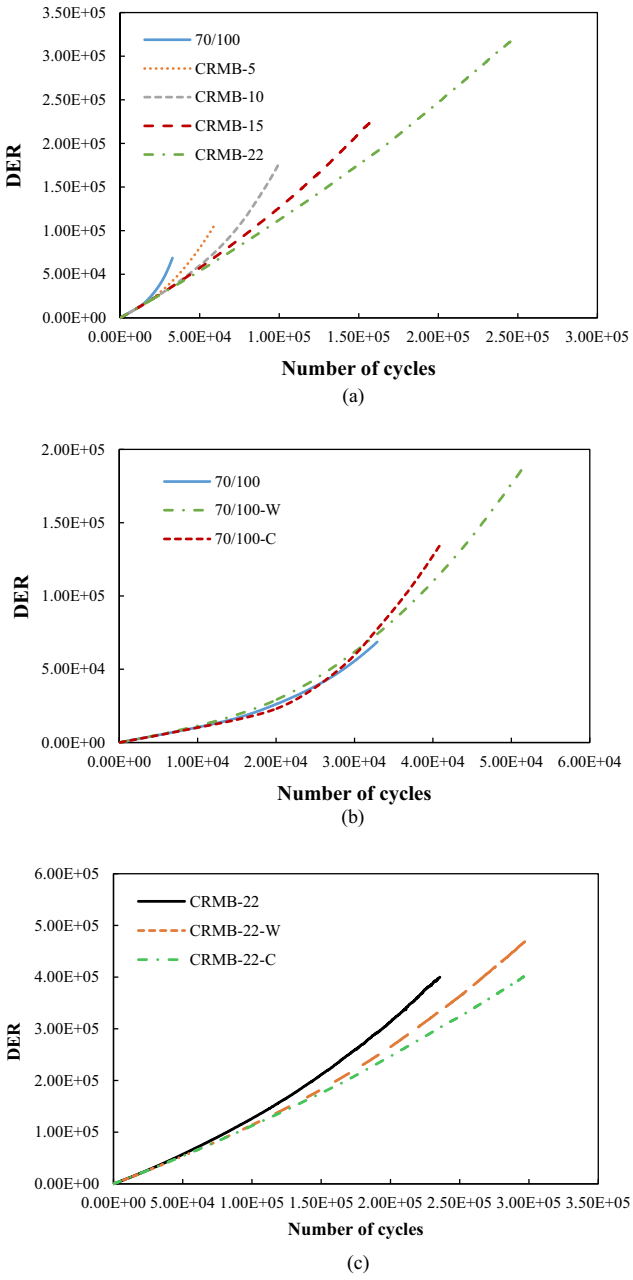

Fig. 8. Plots of DER versus number of load cycles from strain-controlled TS tests at a strain level of 2.5%: (a) CRMB with different CRM contents; (b) base bitumen with warm-mix additives; (c) CRMB with warm-mix additives.

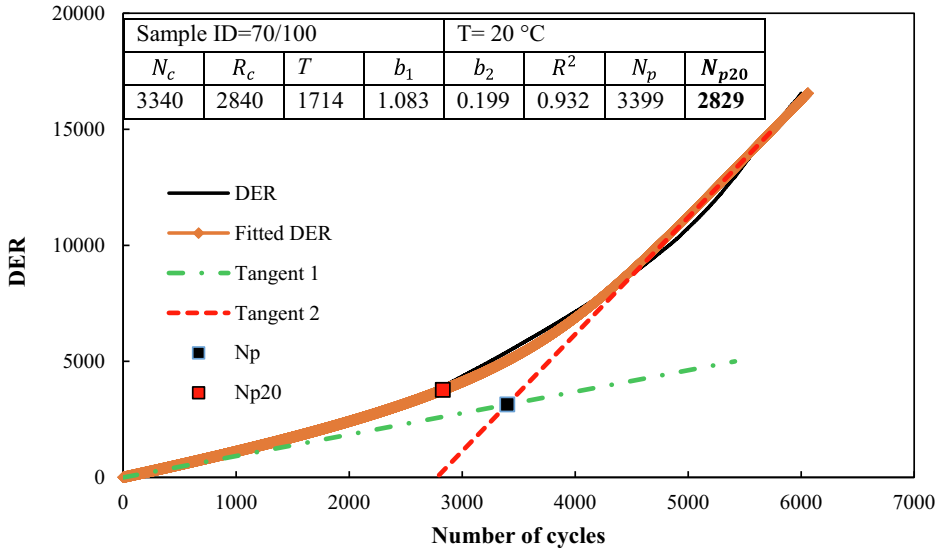

Fig. 9. Modeling of the relationship between DER and number of cycles of neat bitumen at the strain level of 5%.

Table 2
Fatigue life and model parameters from strain-controlled TS tests (20 °C, 10 Hz).

Sample code	Strain level (%)	W_i (Pa)	N_{p20}	K_1	K_2
70/100	2.5	2.05E+04	*1.90E+04*	4.57E+17	1.74E−03
	5.0	2.18E+04	2.83E+03		
70/100-W	2.5	2.29E+04	*1.26E+04*	1.86E+07	3.18E−04
	5.0	2.88E+04	1.96E+03		
70/100-C	2.5	2.12E+04	*2.17E+04*	3.36E+12	9.35E−04
	5.0	2.34E+04	3.07E+03		
CRMB-5	2.5	1.35E+04	*3.43E+04*	5.55E+21	2.93E−03
	5.0	1.43E+04	3.93E+03		
CRMB-10	2.5	1.16E+04	*5.18E+04*	3.17E+10	1.15E−03
	5.0	1.36E+04	5.35E+03		
CRMB-15	2.5	8.93E+03	*8.63E+04*	2.05E+08	8.70E−04
	5.0	1.15E+04	9.25E+03		
CRMB-22	2.5	6.54E+03	*1.15E+05*	1.72E+08	1.12E−03
	5.0	8.51E+03	1.27E+04		
CRMB-22-W	2.5	4.57E+03	*1.45E+05*	7.17E+06	8.54E−04
	5.0	7.12E+03	1.64E+04		
CRMB-22-C	2.5	3.26E+03	*1.81E+05*	3.86E+06	9.38E−04
	5.0	5.63E+03	1.96E+04		

where R represents DER; N_c and R_c are the model constants, representing number of load cycles and dissipated energy ratio respectively; b_1 and b_2 are respectively the slopes of the lower asymptote and upper asymptote of the curve of N versus R; and T is the shape parameter. The solver function in Microsoft Excel was adopted to compute the values of the model parameters using the least-square method. Fig. 9 shows an example of the calculation of the fatigue life N_{p20} of the neat bitumen. Similar procedures were applied to the other binders. For neat bitumen 70/100, the fatigue life N_{p20} at a strain level of 5% is 2829 as summarized in Fig. 9. To obtain the fatigue relationship in Eq. (6), at least two levels of energy input need to be applied. This was achieved by conducting the TS tests at two different strain levels, respectively 2.5% and 5%. The determined fatigue life N_{p20} and fatigue model parameters W_i, K_1 and K_2 of all the tested binders are summarized in Table 2.

It can be seen from Table 2 that the initial energy input W_i has a negative correlation with the fatigue life N_{p20}. Samples with a higher initial energy level have a shorter fatigue life. Measured fatigue life and related model parameters of different binders summarized in Table 2 verified the effects of modifiers on the fatigue performance of base bitumen found from the DER evolution curves. The modification effect on the fatigue properties of base bitumen depends on the modifier's peculiar characteristics and the interaction between the modifier and bitumen. The addition of wax-based additive decreases the (strain controlled) fatigue life of the base bitumen. The wax components form a crystallized structure at 20 °C within the bitumen matrix, which makes the binder stiffer, resulting in higher stresses at a certain strain level, and vulnerable to fatigue damage. The chemical-based additive improves the fatigue resistance of the base bitumen due to the softening effect. The CRM modification significantly prolongs the fatigue life of the base bitumen. The resistance to fatigue damage improves with higher CRM content in the strain-controlled test. Rubber particles are swollen by absorbing aromatic oils from the bitumen during the preparation stage. The interaction between CRM and bitumen results in a three-dimensional polymer network, which prevents or delays formation of microcracks under fatigue loading. Unlike for the neat bitumen, both additives contribute to the improvement of the fatigue performance of CRMB-22 binder. A possible explanation could be that the additives promote the interactions between bitumen and CRM [35].

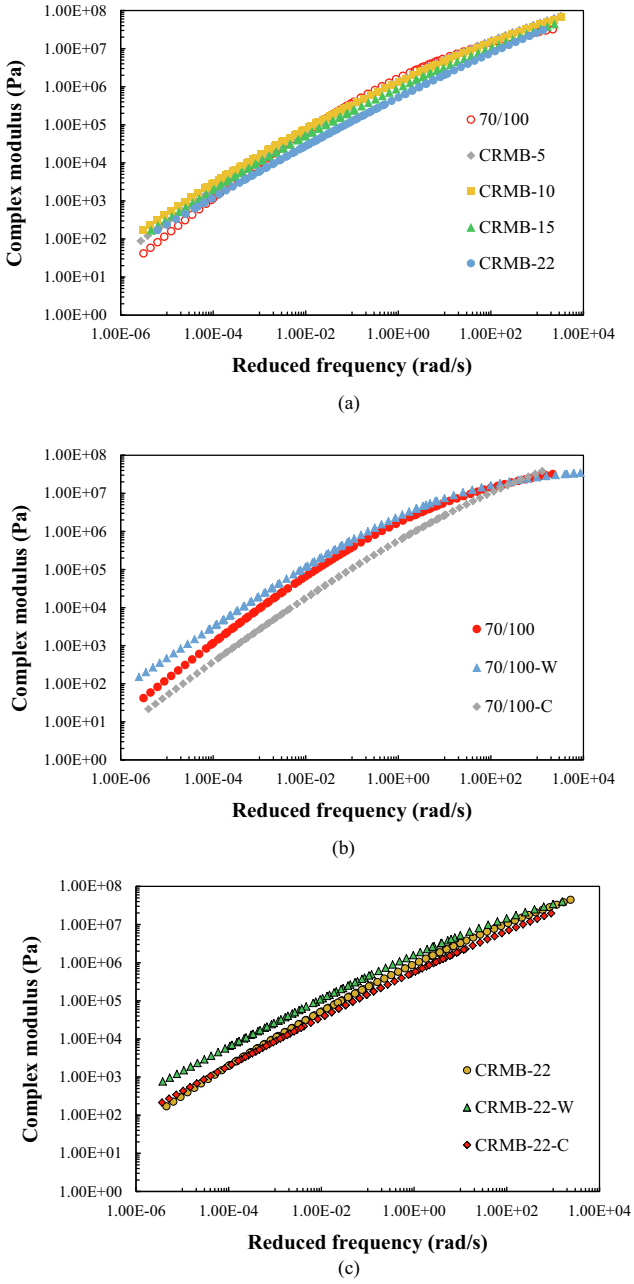

Fig. 10. Complex shear modulus master curves of binders at 20 °C: (a) CRMB with different CRM contents; (b) base bitumen with warm-mix additives; (c) CRMB with warm-mix additives.

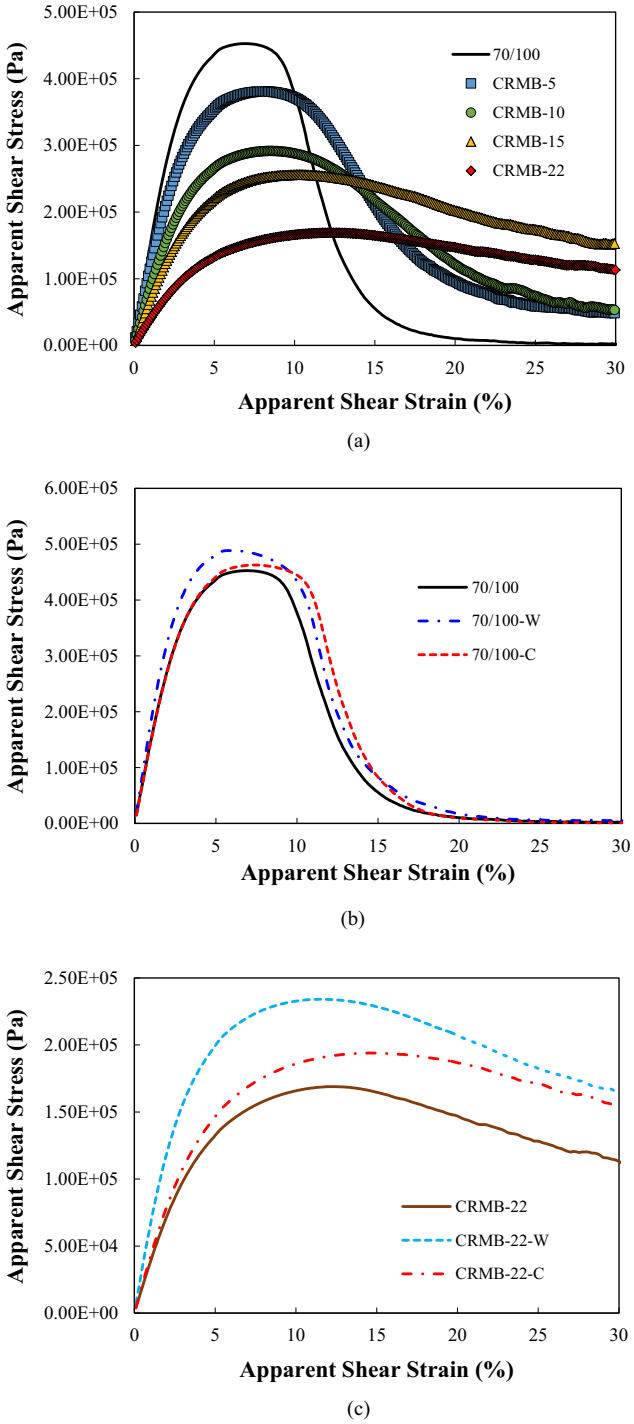

Fig. 11. Apparent stress versus apparent strain from LAS tests: (a) CRMB with different CRM contents; (b) base bitumen with warm-mix additives; (c) CRMB with warm-mix additives.

5.3. LAS test

5.3.1. Linear viscoelastic complex modulus master curves

To obtain the material properties of the binder in the undamaged state, FS tests were performed. Fig. 10 shows the complex shear modulus $|G^*|_{LVE}$ master curves of different binders at the reference temperature of 20 °C. In general, CRMB binders have a higher complex shear modulus than neat bitumen in the low-frequency range, while they have a lower complex shear modulus than the neat bitumen in the high-frequency range at the fatigue testing temperature of 20 °C. This can be explained by the nature of rubber which behaves as an elastic material with a modulus higher than bitumen at high temperatures and lower than bitumen at lower temperatures. It can be seen from Fig. 10a that CRMB-22 has the lowest complex modulus at a frequency of around 62.8 rad/s (10 Hz). With respect to warm-mix additives, the wax-based additive has a consistent stiffening effect on both neat bitumen and CRMB binder, while the chemical-based additive decreases the complex modulus of both neat bitumen and CRMB binder. The reason for this has been explained before by the nature of the additives.

5.3.2. Stress-strain response of different binders

LAS tests were carried out to evaluate the fatigue damage tolerance of binders and were further analyzed using the S-VECD

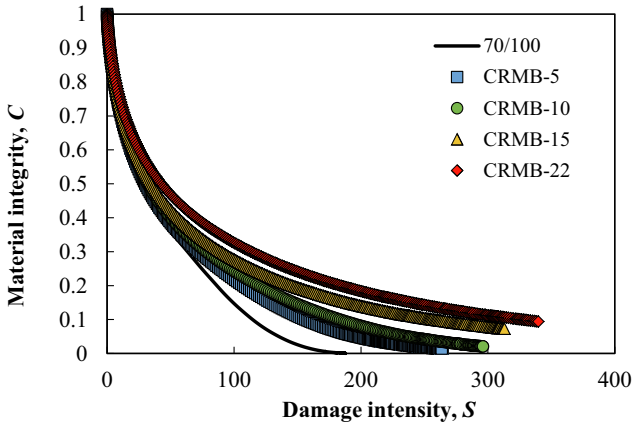

(a)

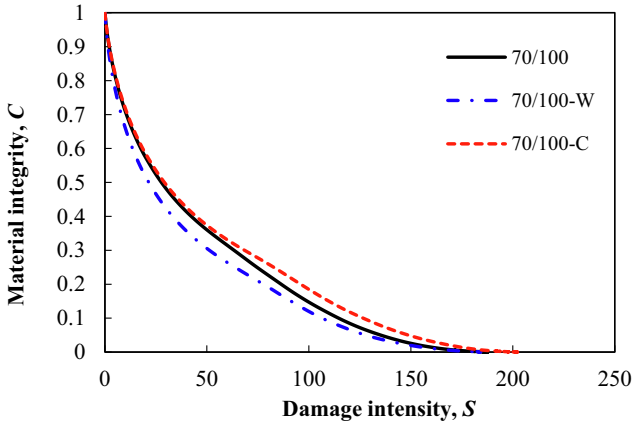

(b)

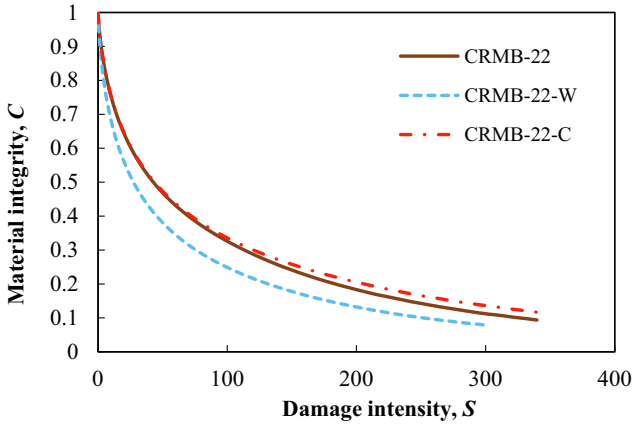

(c)

Fig. 12. Damage characteristic curves of different binders: (a) CRMB with different CRM contents; (b) base bitumen with warm-mix additives; (c) CRMB with warm-mix additives.

model. The apparent shear stress-strain curves of different binders from LAS test results are plotted in Fig. 11. In the initial stage, the shear stress increases linearly with the increase of loading strain. Further increasing the strain amplitude slows down the increase of the shear stress. This is the moment where binders enter the nonlinear regions. Binders reach the peak shear stress at different strain amplitudes. After the peak, the shear stress continuously decreases when further increasing the strain level, indicating significant damage has been induced in the material. It can be seen from Fig. 11a that CRMB binders with a higher CRM content reach the stress peak at a larger strain amplitude. This indicates that CRMB binders with higher CRM contents exhibit higher damage resistance to shear loading. The addition of warm mix additives to neat bitumen changes the strain level at which the peak stress occurs. When reaching the peak shear stress, the corresponding strain for 70/100 is smaller than for 70/100-C, while larger than for 70/100-W. Both additives increase the value of the peak shear stress and the corresponding strain for CRMB-22.

5.3.3. Damage characteristic curves

The stress-strain curves of different binders were further analyzed with the S-VECD model. The damage characteristic curves (C versus S) of different binders are shown in Fig. 12. Different binders show different damage evolution trends related to the resistance to fatigue damage. By fitting the damage characteristic curves using Equation (12), the material integrity of the binder can be determined at any damage intensity of interest. Taking Fig. 12a as an example, at a particular damage intensity, CRMB binders with higher CRM content display higher material integrity, indicating a better fatigue performance. From Fig. 12a and b, the addition of warm-mix additives influences the damage evolution of both neat and CRMB binders in a similar way. However, the damage characteristic curves cannot tell the whole story about the binder fatigue performance. As mentioned before, the S-VECD fatigue characterization includes three material functions, namely the linear viscoelastic properties, damage evolution characteristics and failure criterion. It is inadequate to determine the final fatigue performance merely based on one or two material properties.

5.3.4. Fatigue performance prediction

Fatigue failure point needs to be clearly defined to accurately predict the binder fatigue performance. In addition, a failure criterion needs to be proposed to enable the prediction when the fatigue failure occurs under loading conditions (of interest) that are different from the testing loading conditions.

The proposed definitions of fatigue failure in the LAS test include peak in shear stress, peak in phase angle, peak of $C \times N$ (material integrity times loading cycles), and maximum stored pseudo-strain energy (PSE). It was reported and also found in this study that the variation in phase angle during LAS test in the failure region is minimal, especially for the modified binders. This makes the identification of a fatigue failure point difficult in some cases. In addition, the peak of $C \times N$ defined failure point is always overlapped with the peak stress defined point because $C \times N$ is mathematically relying only on the peak shear stress for a given LAS test condition. Furthermore, the implementation of the failure criterion based on PSE variables requires conducting several LAS tests with different rates of strain amplitude increase [27]. Therefore, for practical and efficient reasons, the current LAS analysis protocol with peak shear stress as the failure point was still used for the fatigue characterization. The damage intensity at failure point S_f is further calculated as

$$S_f = \left(\frac{1 - C_f}{C_1}\right)^{1/C_2} \tag{15}$$

where C_f is the C value at failure, corresponding to the C value when reaching the peak stress in this case. Through combination of Eqs. (15) and (13), the fatigue criterion which describes the relationship between fatigue life N_f and strain amplitude γ_p can be derived as

$$N_f = A\left(\gamma_p\right)^B \tag{16}$$

where A is the model parameter defined in Eq. (17) with $B = -2\alpha$.

$$A = \frac{f \cdot 2^{\alpha} \cdot {S_f}^k}{k(C_1C_2)^{\alpha}(|G^*|_{LVE})^{2\alpha}} \quad (17)$$

where $k = 1 - \alpha C_2 + \alpha$; f is the loading frequency.

With the determined LVE property, damage characteristic curve and fatigue failure criterion, the values of fatigue life and model parameters from LAS tests for different binders are determined (Table 3). Specifically, fatigue life at two strain levels 2.5% and 5% was predicted. It can be found that CRM modification significantly increases the binder fatigue life. Warm-mix additives affect the fatigue life of the base bitumen differently compared to CRMB binder. Both additives improve the fatigue performance of CRMB binder. A possible explanation could be that warm-mix additives enhance the interaction between bitumen and CRM, which makes the binder more resistant to fatigue damage. However, wax-based additive significantly decreases the fatigue life of the base bitumen.

5.4. Fatigue cracking in binders under dynamic shear loading

Above results have demonstrated that CRM and warm-mix additives affect the fatigue resistance of binders in different ways. This is due to the different microstructural compositions of binders. Fig. 13 shows the formation of fatigue cracks in the binder sample under dynamic shear loading. Because of the non-uniform shear stress distribution within the circular binder sample under the applied torque (Fig. 13a), circumferential hairline cracks initiate at the periphery of the sample and then propagate towards the center. Fig. 13b shows a typical cracking morphology of the binder sample on the parallel plate with an annular crack zone and an circular uncrack zone, which is adapted from [13]. A small area in the crack zone was selected as the representative area element to analyze how the microstructures of different binders influence the crack formation. For binders modified with CRM, Fig. 13c shows a swollen rubber particle embedded in the bitumen matrix with a multilayer structure due to the sequential diffusion process of bitumen into rubber [36]. In addition, previous studies have shown that the swollen rubber is softer than bitumen at the intermediate temperature of 20 °C [37]. When the fatigue cracks initiated in the stiff bitumen phase start to propagate, they will encounter the swollen rubber particle. Due to the resemblance between bitumen and the outer layer of the rubber, microcracks will propagate into the rubber. However, because of the polymer network inside the rubber gel, the crack propagation will be delayed. At a larger scale, swollen rubber particles will form a three-dimensional network which can reinforce the binder to have a higher resistance to cracking. This is the reason why CRMB binders have better fatigue performance than neat bitumen. In terms of the neat bitumen modified with wax-based additive, the wax will crystallize at the testing temperature of 20 °C and become very stiff. Stress concentration may occur at the interface between bitumen and wax. When the microcracks meet the wax structure, instead of propagating into the structure, they can only develop into other directions within the bitumen (Fig. 13d), which accelerates the crack formation process. Therefore, binder 70/100-W has a lower cracking resistance than the neat bitumen. With respect to the neat bitumen modified with chemical-based additive, softening effect is believed to be the main reason for improved fatigue resistance. As for the CRMB-22 with wax-based additive, the enhanced interaction between rubber and bitumen due to the existence of wax could be a possible explanation for the improved fatigue performance [35].

5.5. Comparison of binder fatigue parameters

An important objective of this study was to compare the fatigue performance indicators from different fatigue test methods. Fig. 14

Table 3
Fatigue life and model parameters from LAS tests.

Sample code	Parameter A	Parameter B	N_f (@2.5%)	N_f (@5%)
70/100	1.576E+05	−3.285	7.77E+03	7.97E+02
70/100-W	1.464E+05	−3.555	5.63E+03	4.79E+02
70/100-C	2.005E+05	−3.240	1.03E+04	1.09E+03
CRMB-5	5.093E+05	−3.485	2.09E+04	1.87E+03
CRMB-10	6.361E+05	−3.664	2.22E+04	1.75E+03
CRMB-15	1.627E+06	−3.468	6.78E+04	6.12E+03
CRMB-22	1.991E+06	−3.302	9.66E+04	9.80E+03
CRMB-22-W	3.681E+06	−3.631	1.32E+05	1.07E+04
CRMB-22-C	3.843E+06	−3.344	1.80E+05	1.77E+04

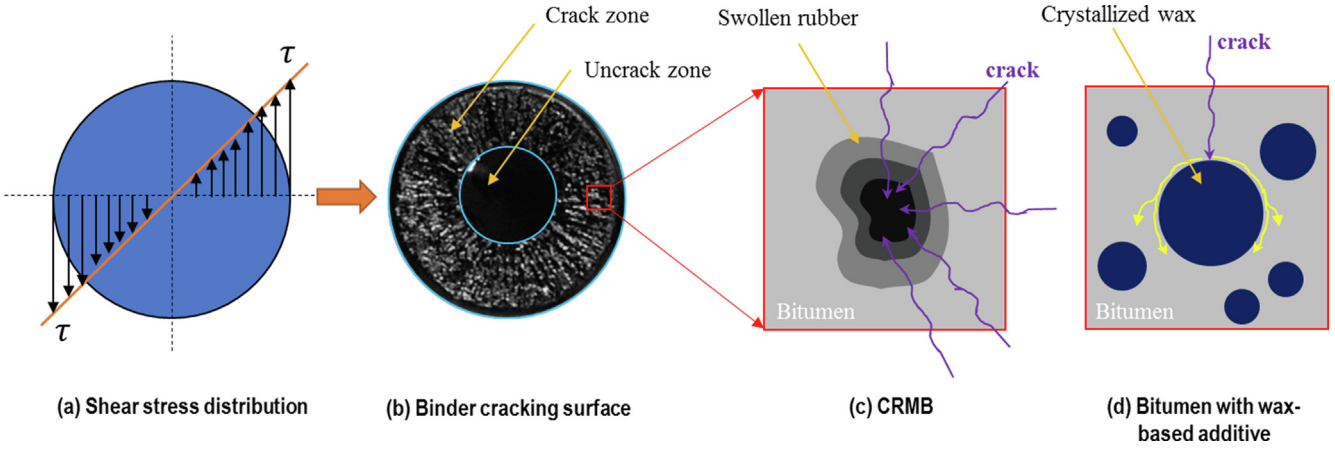

Fig. 13. Fatigue cracking in binders under dynamic shear loading.

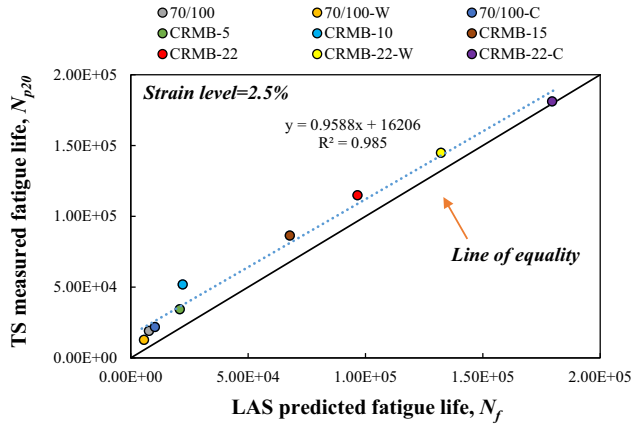

(a)

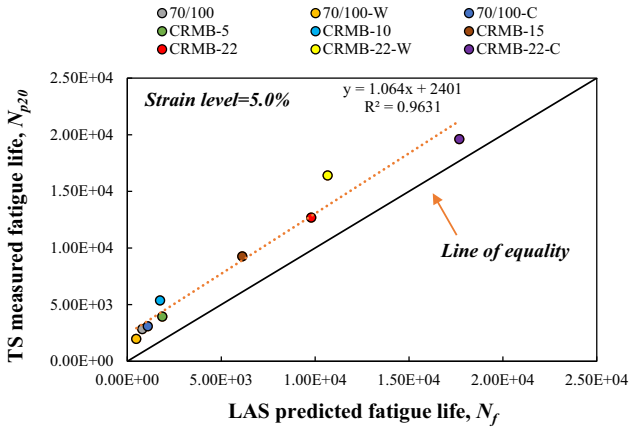

(b)

Fig. 14. Comparison between TS measured fatigue life and LAS predicted fatigue life: (a) at the strain level of 2.5%; (b) at the strain level of 5.0%.

compares the TS measured fatigue life and LAS predicted fatigue life for different binders. There is a good correlation between these two fatigue life values at both strain levels. Generally, for each studied binder, the TS measured fatigue life is longer than the LAS predicted fatigue life at both strain levels. Apparently, this difference in fatigue life of the two methods is related to the different loading mode and rate which affect the fatigue damage accumulation of the binders.

Table 4 summarizes the values of the Superpave fatigue parameter, G-R parameter and fatigue life at the strain level of 2.5% from both TS and LAS tests. The relative ranking of fatigue performance of different binders is also given. A value from 1 to 9 represents the best to worst with respect to fatigue performance. It can be found that TS and LAS tests give the exact same ranking for the fatigue performance of the different binders. The Superpave fatigue parameter ranks the fatigue performance of binders in a similar sequence as TS and LAS tests except for the CRMB-22 with warm-mix additives. However, the ranking of fatigue performance from the G-R parameter is confusing and unreasonable. This is probably because the G-R parameter is a non-load associated parameter and was determined at 15 °C which is different from the fatigue testing temperature. Since TS test results of binders have been proven to have a good correlation with the mixture fatigue performance, they can be taken as the benchmark for characterizing binder fatigue performance. Based on that, the above findings confirm that the LAS test can be used as a good surrogate for the fatigue performance characterization of CRMB-type binders at intermediate temperatures. The Superpave fatigue parameter fails to characterize the fatigue performance when the binder is incorporated with CRM and warm-mix additives. The G-R parameter is not suitable for characterizing the fatigue damage resistance of binders.

6. Conclusions and recommendations

In this study the fatigue performance of long-term aged CRMB containing warm-mix additives was investigated using different fatigue test methods. FS tests were performed to obtain the Superpave fatigue parameter and the G-R parameter, as well as the linear viscoelastic properties of binders which serve as the parameters under undamaged conditions. TS test results were analyzed using the DER concept to determine the binder fatigue life. S-VECD theory was applied in modelling the LAS test results to predict the binder fatigue life. The following conclusions can be drawn based on the test results:

- In terms of the comparison between different fatigue characterization methods, LAS test results correlate well with TS (strain controlled) test results. Both test methods give the same ranking of fatigue life for different binders. The LAS test can be used as an alternative for the TS test to characterize the fatigue performance of CRMB-type binders at intermediate temperatures. The Superpave fatigue parameter performs well, but partly "fails" to characterize the fatigue performance for CRMB with warm-mix additives. The G-R parameter does not seem to be suitable for characterizing the fatigue damage resistance of binders.
- With respect to the effects of CRM modification and warm-mix additives, CRMB binders exhibit superior fatigue performance than the neat bitumen. With the increase of CRM content, the improvement of fatigue life is more significant. The wax-based additive adversely influences the fatigue performance of the neat bitumen while the chemical-based additive improves it. Both additives are beneficial for CRMB-22 with regards to increase of fatigue damage resistance.

Table 4
Binder fatigue performance rankings based on different parameters.

Sample code	G*·sin δ		G-R parameter		N_f (@2.5%) from TS		N_f (@2.5%) from LAS	
	Value (kPa)	Rank	Value (kPa)	Rank	Value	Rank	Value	Rank
70/100	7777	8	12.76	2	1.90E+04	8	7.77E+03	8
70/100-W	7913	9	18.73	3	1.26E+04	9	5.63E+03	9
70/100-C	7219	7	10.87	1	2.17E+04	7	1.03E+04	7
CRMB-5	6751	6	32.08	8	3.43E+04	6	2.09E+04	6
CRMB-10	6356	5	31.23	7	5.18E+04	5	2.22E+04	5
CRMB-15	4256	4	30.15	6	8.63E+04	4	6.78E+04	4
CRMB-22	1901	1	28.94	5	1.15E+05	3	9.66E+04	3
CRMB-22-W	2156	3	34.12	9	1.45E+05	2	1.32E+05	2
CRMB-22-C	2043	2	26.58	4	1.81E+05	1	1.80E+05	1

This study used different fatigue failure criterions for analyzing the TS and LAS test results, a unified failure criterion (e.g., PSE-based analysis) can be applied to the analysis process of both tests in the future. Fatigue performance at the mastic and mixture levels should be also evaluated to verify the findings at the binder level.

CRediT authorship contribution statement

Haopeng Wang: Conceptualization, investigation, methodology, Writing - original draft, Writing-review and editing. **Xueyan Liu**: Methodology, Investigation. **Martin van de Ven**: methodology, Writing-review and editing. **Guoyang Lu**: Investigation, Visualization. **Sandra Erkens**: Data curation, Supervision. **Athanasios Skarpas**: Project administration, Supervision.

Declaration of Competing Interest

The authors declare that they have no known competing financial interests or personal relationships that could have appeared to influence the work reported in this paper.

Acknowledgements

The corresponding author thanks the financial support from the China Scholarship Council. The financial support of Khalifa University via the CIRA-2018-115 research grant is also gratefully acknowledged.

References

[1] WBCSD, End-of-Life Tires: A framework for effective management systems, in: W.B.C.f.S. Development (Ed.) World Business Council for Sustainable Development, Conches-Geneva, Switzerland, 2010.
[2] K. Stevenson, B. Stallwood, A.G. Hart, Tire rubber recycling and bioremediation: a review, Biorem. J. 12 (1) (2008) 1–11.
[3] D. Lo Presti, Recycled tyre rubber modified bitumens for road asphalt mixtures: a literature review, Constr. Build. Mater. 49 (2013) 863–881.
[4] H. Wang, X. Liu, H. Zhang, P. Apostolidis, T. Scarpas, S. Erkens, Asphalt-rubber interaction and performance evaluation of rubberised asphalt binders containing non-foaming warm-mix additives, Road Mater. Pavem. Design (2018) 1–22.
[5] H. Wang, X. Liu, P. Apostolidis, T. Scarpas, Non-Newtonian behaviors of crumb rubber-modified bituminous binders, Appl. Sci. 8 (10) (2018) 1760.
[6] F. Farshidi, D. Jones, J.T. Harvey, Warm-Mix Asphalt Study: Evaluation of Rubberized Hot- and Warm-Mix Asphalt with Respect to Emissions, Research Report: UCPRC-RR-2013-03, University of California Pavement Research Center, Davis, California, USA, 2013.
[7] G.L. Baumgardner, G.R. Reinke, Binder additives for warm mix asphalt technology, J. Assoc. Asphalt Paving Technol. 82 (2013) 685–709.
[8] T. Bennert, G. Reinke, W. Mogawer, K. Mooney, Assessment of workability and compactability of warm-mix asphalt, Transport. Res. Record: J. Transp. Res. Board 2180 (2010) 36–47.
[9] A.J. Hanz, A. Faheem, E. Mahmoud, H.U. Bahia, Measuring effects of warm-mix additives use of newly developed asphalt binder lubricity test for the dynamic shear rheometer, Transp. Res. Record 2180 (2180) (2010) 85–92.
[10] H. Wang, X. Liu, P. Apostolidis, T. Scarpas, Review of warm mix rubberized asphalt concrete: towards a sustainable paving technology, J. Cleaner Prod. 177 (2018) 302–314.
[11] R. Cao, Z. Leng, H. Yu, S.-C. Hsu, Comparative life cycle assessment of warm mix technologies in asphalt rubber pavements with uncertainty analysis, Resour. Conserv. Recycl. 147 (2019) 137–144.
[12] H. Yu, Z. Leng, Z. Zhou, K. Shih, F. Xiao, Z. Gao, Optimization of preparation procedure of liquid warm mix additive modified asphalt rubber, J. Cleaner Prod. 141 (2017) 336–345.
[13] Y. Zhang, Y. Gao, Predicting crack growth in viscoelastic bitumen under a rotational shear fatigue load, Road Mater. Pavem. Des. (2019) 1–20.
[14] Y. Gao, Y. Zhang, Y. Yang, J. Zhang, F. Gu, Molecular dynamics investigation of interfacial adhesion between oxidised bitumen and mineral surfaces, Appl. Surf. Sci. 479 (2019) 449–462.
[15] R. Hajj, A. Bhasin, The search for a measure of fatigue cracking in asphalt binders – a review of different approaches, Int. J. Pavement Eng. 19 (3) (2017) 205–219.
[16] D.A. Anderson, T.W. Kennedy, Development of SHRP binder specification, J. Assoc. Asphalt Paving Technol. 62 (1993) 481–507.
[17] H.U. Bahia, H. Zhai, K. Onnetti, S. Kose, Non-linear viscoelastic and fatigue properties of asphalt binders, J. Assoc. Asphalt Paving Technol. 68 (1999) 1–34.
[18] H.U. Bahia, H. Zhai, M. Zeng, Y. Hu, P. Turner, Development of binder specification parameters based on characterization of damage behavior, J. Assoc. Asphalt Paving Technol. 70 (2001) 442–470.
[19] G.M. Rowe, G. King, M. Anderson, The influence of binder rheology on the cracking of asphalt mixes in airport and highway projects, J. Test. Eval. 42 (5) (2014) 20130245.
[20] R.M. Anderson, G.N. King, D.I. Hanson, P.B. Blankenship, Evaluation of the relationship between asphalt binder properties and non-load related cracking, J. Assoc. Asphalt Paving Technol. 80 (2011).
[21] H.U. Bahia, D.I. Hanson, M. Zeng, H. Zhai, M.A. Khatri, R.M. Anderson, Characterization of Modified Asphalt Binders in Superpave Mix Design, NCHRP Report 459, Transportation Research Board, Washington D.C, 2001.
[22] D.A. Anderson, Y.M. Le Hir, M.O. Marasteanu, J.P. Planche, D. Martin, G. Gauthier, Evaluation of fatigue criteria for asphalt binders, Transp. Res. Record 1766 (2001) 48–56.
[23] C. Wang, H. Zhang, C. Castorena, J. Zhang, Y.R. Kim, Identifying fatigue failure in asphalt binder time sweep tests, Constr. Build. Mater. 121 (2016) 535–546.
[24] K.S. Bonnetti, K. Nam, H.U. Bahia, Measuring and defining fatigue behavior of asphalt binders, Transp Res Record 2002 (1810) 33–43.
[25] R. Delgadillo, H. Bahia, Rational fatigue limits for asphalt binders derived from pavement analysis, J. Assoc. Asphalt Paving Technol. 78 (2005) 97–138.
[26] W. Cao, C. Wang, A new comprehensive analysis framework for fatigue characterization of asphalt binder using the Linear Amplitude Sweep test, Constr. Build. Mater. 171 (2018) 1–12.
[27] C. Wang, C. Castorena, J. Zhang, Y. Richard Kim, Unified failure criterion for asphalt binder under cyclic fatigue loading, Road Mater. Pavem. Design 16 (sup2) (2015) 125–148.
[28] C. Hintz, R. Velasquez, C. Johnson, H. Bahia, Modification and validation of linear amplitude sweep test for binder fatigue specification, Transp. Res. Record: J. Transp. Res. Board 2207 (2011) 99–106.
[29] C. Hintz, H. Bahia, Understanding mechanisms leading to asphalt binder fatigue in the dynamic shear rheometer, Road Mater. Pavem. Design 14 (sup2) (2013) 231–251.
[30] F. Safaei, C. Castorena, Temperature effects of linear amplitude sweep testing and analysis, Transp. Res. Record: J. Transp. Res Board 2574 (2016) 92–100.
[31] H. Wang, X. Liu, P. Apostolidis, T. Scarpas, Rheological behavior and its chemical interpretation of crumb rubber modified asphalt containing warm-mix additives, Transp. Res. Record: J. Transp. Res. Board 2672 (28) (2018) 337–348.
[32] B.S. Underwood, C. Baek, Y.R. Kim, Simplified viscoelastic continuum damage model as platform for asphalt concrete fatigue analysis, Transp. Res. Record 2296 (2012) 36–45.
[33] R. Schapery, Analysis of damage growth in particulate composites using a work potential, Compos. Eng. 1 (3) (1991) 167–182.
[34] F. Safaei, J.-S. Lee, L.A.H.D. Nascimento, C. Hintz, Y.R. Kim, Implications of warm-mix asphalt on long-term oxidative ageing and fatigue performance of asphalt binders and mixtures, Road Mater. Pavem. Des. 15 (sup1) (2014) 45–61.
[35] H. Yu, Z. Leng, Z. Gao, Thermal analysis on the component interaction of asphalt binders modified with crumb rubber and warm mix additives, Constr. Build. Mater. 125 (2016) 168–174.
[36] H. Wang, X. Liu, P. Apostolidis, S. Erkens, T. Scarpas, Numerical investigation of rubber swelling in bitumen, Constr. Build. Mater. 214 (2019) 506–515.
[37] H. Wang, X. Liu, P. Apostolidis, S. Erkens, A. Skarpas, Experimental investigation of rubber swelling in bitumen, Transp. Res. Record: J. Transp. Res. Board (2020). Submitted.